temperature. Fetal spleen morphology was assessed using an Olympus CKX41 inverted microscope, an Olympus DP71 microscope digital camera and image capture software (DP manager version 3.1.1.208 and DP controller 3.2.1.276, Olympus, Tokyo, Japan).

Cell preparation

Fetal spleens or livers at 16.5 dpc and 19.5 dpc were dissected as described above. To prepare single cell suspensions, fetal spleens or livers were incubated with 3 mg/mL collagenase type 1 (Worthington Biochemical Corporation, New Jersey) in medium supplemented with 10% fetal bovine serum for 30 minutes at 37℃ and passed through 70-μm nylon cell strainers (BD Biosciences, California).

Flow cytometry and cell sorting

Antibodies used for analysis were: Pacific Blue-, APC- and PE-Cy7-conjugated anti-mouse CD45; PE-Cy7-, APC-Cy7- and APC-conjugated anti-mouse Ter119; PE- and APC-conjugated anti-mouse CD31; APC-conjugated anti-mouse LYVE-1; FITC-conjugated anti-mouse DLK-1; PE-Cy7-conjugated anti-mouse CD106; PE-conjugated anti-mouse CD51; PE-conjugated anti-mouse CD73; PE-conjugated anti-mouse CD105; PE-conjugated anti-mouse CD166; PE-conjugated anti-mouse CD44; FITC-conjugated anti-mouse CD29; FITC-conjugated anti-mouse CD90.2; Biotin-conjugated CD144a; FITC-conjugated streptavidin; FITC-conjugated anti-mouse c-Kit; rabbit-anti-mouse IGF-1R; Alexa Fluor®488 donkey anti-rabbit IgG ; PE-conjugated anti-mouse Sca-1; APC-conjugated anti-mouse c-Kit and FITC-conjugated anti-mouse CD71. Antibodies were purchased from eBioscience, San Diego, CA; BioLegend, San Diego, CA; Invitrogen, Carlsbad, CA; and MBL, Nagoya, Japan. Flow cytometric analysis and cell sorting were carried out using a FACSAria SORP cell sorter (BDIS, San Jose, CA). Data files were analyzed using FlowJo software (Tree Star, Inc., San Carlos, CA).

RNA extraction and real-time PCR analysis

Total RNA was isolated using the RNAqueous®-4PCR kit (Ambion Inc., Austin, Texas) and a RiboPure™ RNA Purification Kit (Ambion Inc.). mRNA was reverse transcribed using a high-capacity RNA-to-cDNA kit (Life Technologies, Carlsbad, CA). Gene expression levels were measured by real-time PCR (StepOnePlus™ real-time PCR; Life Technologies) with TaqMan® Gene Expression Master Mix (Life Technologies). Primers and probes for *Stem cell factor* (*Scf*) (Mm00442972_m1), *Insulin-like growth factor 1* (*Igf1*) (Mm00439560_m1), *Interleukin-3* (*Il-3*) (Mm00439631_m1), *Erythropoietin* (*Epo*) (Mm00433126_m1), *GATA-binding factor 1* (*Gata1*) (Mm01352636_m1), *Kruppel-like factor 1* (*Klf1*) (Mm00516096_m1) and *β-major globin* (*Hbb-b1*) (Mm01611268_g1) were from TaqMan® Gene Expression Assays (Life Technologies). The thermal protocol was set to 2 minutes at 50℃, followed by 10 minutes at 95℃, and then 40 cycles of 15 seconds at 95℃ and 1 minute at 60℃. *β-actin* (Mm00607939_s1) served as internal control. All analyses were performed in triplicate; mRNA levels were normalized to *β-actin* and relative expression (RQ) was compared with a reference sample.

Enzyme-linked immunosorbent assay (ELISA)

Lysates of whole fetal spleen or liver tissues were prepared using the Qproteome Mammalian Protein Prep Kit (Qiagen, Hilden, Germany), according to the manufacturer's instructions. Hematopoietic cells (CD45+/CD45+Ter119+/Ter119+), endothelial cells (CD45−Ter119−CD31+LYVE-1−), unclassified cells (CD45−Ter119−CD31−LYVE-1−) and CD51+ cells among unclassified cells (CD45−Ter119−CD31−LYVE-1−CD51+) were sorted. Lysates were prepared using M-PER Mammalian Protein Extraction Reagent (Thermo Fisher Scientific, Rockford, IL) and a protease inhibitor from the Qproteome Mammalian Protein Prep Kit (Qiagen). Samples were centrifuged at 12,000 rpm for 10 minutes at 4℃. Supernatants containing soluble protein were collected and protein concentration was quantitated using the Bradford reagent (Bio Rad, Hercules, CA) according to the manufacturer's instruction. The optical density (O.D.) at 540 nm was measured using a Thermo Multiskan FC plate reader (Thermo Fisher Scientific). SCF, IGF-1, IL-3 and EPO ELISA assays were conducted using a mouse SCF Quantikine ELISA kit (R&D Systems, Minneapolis, MN), a mouse IGF-1 Quantikine ELISA kit (R&D Systems), a mouse IL-3 Quantikine ELISA kit (R&D Systems) and a mouse EPO Quantikine ELISA kit (R&D Systems), according to the manufacturer's instructions. O.D.s at 450 nm and 540 nm were measured using a Thermo Multiskan FC plate reader.

Immunohistochemistry

Frozen blocks of 16.5 dpc fetal spleen at were prepared, and 10 μm sections were cut using a Leica CM1900 UV cryostat, transferred to glass slides (Matsunami, Osaka, Japan) and dried thoroughly. Sections were washed three times with PBS, blocked with 1% BSA in PBS and incubated with appropriate dilutions of the following primary antibodies at 4℃ overnight: 1:300 anti-mouse CD31 rat IgG (MEC13.3; BD Biosciences, San Diego, CA), 1:300 anti-mouse CD51 rat IgG (RMV-7; BD Biosciences), 1:300 anti-mouse LYVE-1 rat IgG (ALY7; MBL, Woburn, MA) and 1:300 anti-mouse DLK-1 rat IgG (24-11; MBL). In addition, a Tyramide Signal Amplification System (PerkinElmer, Waltham, Massachusetts) was used for SCF and IGF-1 detection in 16.5 dpc fetal spleen using appropriate dilutions of the following primary antibodies: anti-mouse SCF goat IgG (sc-1303; Santa Cruz Biotechnology) and anti-mouse IGF-1 goat IgG (AF791; R&D systems), both at 4℃ overnight. After three PBS washes, sections were incubated with appropriate dilutions of the following secondary antibodies: Alexa Fluor®488 donkey anti-rat IgG (Invitrogen, Carlsbad, CA), HRP donkey anti-goat IgG (R&D systems), Alexa Fluor®546 Streptavidin (Invitrogen) as well as TOTO-3 (Invitrogen) to stain nuclei, at room temperature for 30 minutes. Samples were mounted on slides using fluorescent mounting medium (Dako Corporation), covered with cover glass, and assessed using a FluoView 1000 Confocal Microscope (Olympus).

Co-culture of stromal and hematopoietic cells

For co-culture, whole fetal spleen cells were dissociated into single cells and cultured on 0.1% gelatin-coated tissue culture plate. After two hours, cells that had adhered to the plate were used as stromal cells. Non-adherent cells containing hematopoietic cells were collected and cultured with stromal cells in StemPro®-34 serum-free medium (SFM) (Gibco, Invitrogen, Carlsbad, CA) at 37℃ and 5% CO_2. After 24 hours of culture, cells were collected and assessed by flow cytometry after staining with the following antibodies: PB-conjugated anti-mouse CD45, APC-conjugated anti-mouse c-Kit, PE-conjugated anti-mouse CD71 and PE-Cy7-conjugated anti-mouse Ter119.

In vitro functional assay

Whole fetal spleen cells were prepared as described above and cultured with StemPro®-34 SFM in the presence of the SCF inhibitor ISCK03 (10 μM) (sc-355981, Santa Cruz Biotechnology), the IGF-1R inhibitor PPP (10 μM) (sc-204008, Santa Cruz Biotechnology) or both (10 μM each). DMSO (Wako Pure Chemical Industries) served as a vehicle control at a final concentration of less than 0.1%. After 24 hours of culture, cells were stained with PB-conjugated anti-mouse CD45, APC-conjugated anti-mouse c-Kit and PE-Cy7-conjugated anti-mouse Ter119 and analyzed by flow cytometry.

In vivo functional assay

Pregnant ICR mice at 16.5 dpc were intravenously injected with DMSO (control), the SCF inhibitor (1.56 μg/g body weight), the IGF-1R inhibitor (1.92 μg/g body weight) or both. Two hours later, fetal spleens from embryos were dissected and single cell suspensions were prepared as described.

Statistical analysis

Data were presented as means±standard deviation (SD). Student's *t*-test was used to calculate statistical significance. A P value less than 0.05 was considered statistically significant.

Acknowledgements

We thank Ms. Wai Feng Lim and Chiyo Mizuochi-Yanagi for discussion and technical support, Drs. Yoichi Nakanishi, Elizabeth George and Syahrilnizam

Abdullah for continuous encouragement and Dr. Elise Lamar for critical reading of the manuscript.

Competing interests
The authors declare no competing or financial interests.

Author contributions
D.S. and M.I.L. conceived the study. D.S. designed the experiments, interpreted the data, and prepared the manuscript. K.S.T. performed the experiments and participated in data interpretation and manuscript preparation. T.I., K.K. and Y.T. assisted in data analysis and manuscript preparation.

Funding
This work was supported by grants from the Ministry of Education, Culture, Sports, Science and Technology; the Ministry of Health, Labor and Welfare; the *Japan Society for the Promotion of Science*; *the Ichiro Kanehara Foundation for* the Promotion of Medical Sciences and Medical Care; the Institute of Molecular Embryology and Genetics; and the International Research Fund for Subsidy of Kyushu University School of Medicine Alumni. Keai Sinn Tan is a recipient of a scholarship from the Tokyo Biochemical Research Foundation, Japan, and a MyPhD scholarship from Ministry of Higher Education (MOHE), Malaysia.

References
Ayres-Silva, J. P., Manso, P. P. D., Madeira, M. R. D., Pelajo-Machado, M. and Lenzi, H. L. (2011). Sequential morphological characteristics of murine fetal liver hematopoietic microenvironment in Swiss Webster mice. *Cell Tissue Res.* **344**, 455-469.

Bertrand, J. Y., Giroux, S., Golub, R., Klaine, M., Jalil, A., Boucontet, L., Godin, I. and Cumano, A. (2005). Characterization of purified intraembryonic hematopoietic stem cells as a tool to define their site of origin. *Proc. Natl. Acad. Sci. USA* **102**, 134-139.

Bertrand, J. Y., Desanti, G. E., Lo-Man, R., Leclerc, C., Cumano, A. and Golub, R. (2006). Fetal spleen stroma drives macrophage commitment. *Development* **133**, 3619-3628.

Chou, S. and Lodish, H. F. (2010). Fetal liver hepatic progenitors are supportive stromal cells for hematopoietic stem cells. *Proc. Natl. Acad. Sci. USA* **107**, 7799-7804.

Dai, C. H., Krantz, S. B. and Zsebo, K. M. (1991). Human burst-forming units-erythroid need direct interaction with stem cell factor for further development. *Blood* **78**, 2493-2497.

Desanti, G. E., Cumano, A. and Golub, R. (2008). Identification of CD4int progenitors in mouse fetal spleen, a source of resident lymphoid cells. *J. Leukoc. Biol.* **83**, 1145-1154.

Djaldetti, M., Bessler, H. and Rifkind, R. A. (1972). Hematopoiesis in the embryonic mouse spleen: an electron microscopic study. *Blood* **39**, 826-841.

Ema, H. and Nakauchi, H. (2000). Expansion of hematopoietic stem cells in the developing liver of a mouse embryo. *Blood* **95**, 2284-2288.

Emerson, S. G., Thomas, S., Ferrara, J. L. and Greenstein, J. L. (1989). Developmental regulation of erythropoiesis by hematopoietic growth factors: analysis on populations of BFU-E from bone marrow, peripheral blood, and fetal liver. *Blood* **74**, 49-55.

Giuliani, M., Fleury, M., Vernochet, A., Ketroussi, F., Clay, D., Azzarone, B., Lataillade, J. J. and Durrbach, A. (2011). Long-lasting inhibitory effects of fetal liver mesenchymal stem cells on T-lymphocyte proliferation. *PLoS ONE* **6**, e19988.

Godin, I., Garcia-Porrero, J. A., Dieterlen-Lièvre, F. and Cumano, A. (1999). Stem cell emergence and hemopoietic activity are incompatible in mouse intraembryonic sites. *J. Exp. Med.* **190**, 43-52.

Goodman, J. W., Hall, E. A., Miller, K. L. and Shinpock, S. G. (1985). Interleukin 3 promotes erythroid burst formation in "serum-free" cultures without detectable erythropoietin. *Proc. Natl. Acad. Sci. USA* **82**, 3291-3295.

Green, M. C. (1967). A defect of the splanchnic mesoderm caused by the mutant gene dominant hemimelia in the mouse. *Dev. Biol.* **15**, 62-89.

Guo, Y., Zhang, X., Huang, J., Zeng, Y., Liu, W., Geng, C., Li, K. W., Yang, D., Wu, S., Wei, H. et al. (2009). Relationships between hematopoiesis and hepatogenesis in the midtrimester fetal liver characterized by dynamic transcriptomic and proteomic profiles. *PLoS ONE* **4**, e7641.

Hinton, R., Petvises, S. and O'Neill, H. (2011). Myelopoiesis related to perinatal spleen. *Immunol. Cell Biol.* **89**, 689-695.

Houlihan, D. D., Mabuchi, Y., Morikawa, S., Niibe, K., Araki, D., Suzuki, S., Okano, H. and Matsuzaki, Y. (2012). Isolation of mouse mesenchymal stem cells on the basis of expression of Sca-1 and PDGFR-α. *Nat. Protoc.* **7**, 2103-2111.

Houssaint, E. (1981). Differentiation of the mouse hepatic primordium. II. Extrinsic origin of the haemopoietic cell line. *Cell Differ.* **10**, 243-252.

Inoue, T., Sugiyama, D., Kurita, R., Oikawa, T., Kulkeaw, K., Kawano, H., Miura, Y., Okada, M., Suehiro, Y., Takahashi, A. et al. (2011). APOA-1 is a novel marker of erythroid cell maturation from hematopoietic stem cells in mice and humans. *Stem Cell Rev.* **7**, 43-52.

Ji, P., Jayapal, S. R. and Lodish, H. F. (2008). Enucleation of cultured mouse fetal erythroblasts requires Rac GTPases and mDia2. *Nat. Cell Biol.* **10**, 314-321.

Kina, T., Ikuta, K., Takayama, E., Wada, K., Majumdar, A. S., Weissman, I. L. and Katsura, Y. (2000). The monoclonal antibody TER-119 recognizes a molecule associated with glycophorin A and specifically marks the late stages of murine erythroid lineage. *Br. J. Haematol.* **109**, 280-287.

Kingsley, P. D., Malik, J., Fantauzzo, K. A. and Palis, J. (2004). Yolk sac-derived primitive erythroblasts enucleate during mammalian embryogenesis. *Blood* **104**, 19-25.

Kodama, H., Nose, M., Niida, S., Nishikawa, S. and Nishikawa, S. (1994). Involvement of the c-kit receptor in the adhesion of hematopoietic stem cells to stromal cells. *Exp. Hematol.* **22**, 979-984.

Koury, M. J. and Bondurant, M. C. (1992). The molecular mechanism of erythropoietin action. *Eur. J. Biochem.* **210**, 649-663.

Li, T. and Wu, Y. (2011). Paracrine molecules of mesenchymal stem cells for hematopoietic stem cell niche. *Bone Marrow Res.* **2011**, 353878.

Li, M. O., Sanjabi, S. and Flavell, R. A. (2006). Transforming growth factor-beta controls development, homeostasis, and tolerance of T cells by regulatory T cell-dependent and -independent mechanisms. *Immunity* **25**, 455-471.

McGrath, K. and Palis, J. (2008). Ontogeny of erythropoiesis in the mammalian embryo. *Curr. Top. Dev. Biol.* **82**, 1-22.

Miyagawa, S., Kobayashi, M., Konishi, N., Sato, T. and Ueda, K. (2000). Insulin and insulin-like growth factor I support the proliferation of erythroid progenitor cells in bone marrow through the sharing of receptors. *Br. J. Haematol.* **109**, 555-562.

Morrison, S. J., Hemmati, H. D., Wandycz, A. M. and Weissman, I. L. (1995). The purification and characterization of fetal liver hematopoietic stem cells. *Proc. Natl. Acad. Sci. USA* **92**, 10302-10306.

Munugalavadla, V. and Kapur, R. (2005). Role of c-Kit and erythropoietin receptor in erythropoiesis. *Crit. Rev. Oncol. Hematol.* **54**, 63-75.

Muta, K., Krantz, S. B., Bondurant, M. C. and Wickrema, A. (1994). Distinct roles of erythropoietin, insulin-like growth factor I, and stem cell factor in the development of erythroid progenitor cells. *J. Clin. Invest.* **94**, 34-43.

Nakano, T., Kodama, H. and Honjo, T. (1994). Generation of lymphohematopoietic cells from embryonic stem cells in culture. *Science* **265**, 1098-1101.

Neubauer, K., Wilfling, T., Ritzel, A. and Ramadori, G. (2000). Platelet-endothelial cell adhesion molecule-1 gene expression in liver sinusoidal endothelial cells during liver injury and repair. *J. Hepatol.* **32**, 921-932.

Ohls, R. K., Li, Y., Trautman, M. S. and Christensen, R. D. (1994). Erythropoietin production by macrophages from preterm infants: implications regarding the cause of the anemia of prematurity. *Pediatr. Res.* **35**, 169-170.

Ohno, H., Ogawa, M., Nishikawa, S., Hayashi, S., Kunisada, T. and Nishikawa, S. (1993). Conditions required for myelopoiesis in murine spleen. *Immunol. Lett.* **35**, 197-204.

Palis, J. (2014). Primitive and definitive erythropoiesis in mammals. *Front. Physiol.* **5**, 3.

Palis, J., Robertson, S., Kennedy, M., Wall, C. and Keller, G. (1999). Development of erythroid and myeloid progenitors in the yolk sac and embryo proper of the mouse. *Development* **126**, 5073-5084.

Patterson, K. D., Drysdale, T. A. and Krieg, P. A. (2000). Embryonic origins of spleen asymmetry. *Development* **127**, 167-175.

Pinho, S., Lacombe, J., Hanoun, M., Mizoguchi, T., Bruns, I., Kunisaki, Y. and Frenette, P. S. (2013). PDGFRα and CD51 mark human nestin+ sphere-forming mesenchymal stem cells capable of hematopoietic progenitor cell expansion. *J. Exp. Med.* **210**, 1351-1367.

Sadahira, Y., Yasuda, T., Yoshino, T., Manabe, T., Takeishi, T., Kobayashi, Y., Ebe, Y. and Naito, M. (2000). Impaired splenic erythropoiesis in phlebotomized mice injected with CL2MDP-liposome: an experimental model for studying the role of stromal macrophages in erythropoiesis. *J. Leukoc. Biol.* **68**, 464-470.

Sasaki, K. and Matsumura, G. (1987). Hemopoietic cells in the liver and spleen of the embryonic and early postnatal mouse: a karyometrical observation. *Anat. Rec.* **219**, 378-383.

Sasaki, K. and Matsumura, G. (1988). Spleen lymphocytes and haemopoiesis in the mouse embryo. *J. Anat.* **160**, 27-37.

Socolovsky, M., Nam, H., Fleming, M. D., Haase, V. H., Brugnara, C. and Lodish, H. F. (2001). Ineffective erythropoiesis in Stat5a(-/-)5b(-/-) mice due to decreased survival of early erythroblasts. *Blood* **98**, 3261-3273.

Sugiyama, D., Inoue-Yokoo, T., Fraser, S. T., Kulkeaw, K., Mizuochi, C. and Horio, Y. (2011a). Embryonic regulation of the mouse hematopoietic niche. *ScientificWorldJournal* **11**, 1770-1780.

Sugiyama, D., Kulkeaw, K., Mizuochi, C., Horio, Y. and Okayama, S. (2011b). Hepatoblasts comprise a niche for fetal liver erythropoiesis through cytokine production. *Biochem. Biophys. Res. Commun.* **410**, 301-306.

Suire, C., Brouard, N., Hirschi, K. and Simmons, P. J. (2012). Isolation of the stromal-vascular fraction of mouse bone marrow markedly enhances the yield of clonogenic stromal progenitors. *Blood* **119**, e86-e95.

Tan, K. S., Tamura, K., Lai, M. I., Veerakumarasivam, A., Nakanishi, Y., Ogawa, M. and Sugiyama, D. (2013). Molecular pathways governing development of vascular endothelial cells from ES/iPS cells. *Stem Cell Rev.* **9**, 586-598.

Udupa, K. B. and Reissmann, K. R. (1979). In vivo erythropoietin requirements of regenerating erythroid progenitors (BFU-e, CFU-e) in bone marrow of mice. *Blood* **53**, 1164-1171.

Umemura, T., al-Khatti, A., Donahue, R. E., Papayannopoulou, T. and Stamatoyannopoulos, G. (1989). Effects of interleukin-3 and erythropoietin on in vivo erythropoiesis and F-cell formation in primates. *Blood* **74**, 1571-1576.

Wang, X., Hisha, H., Taketani, S., Adachi, Y., Li, Q., Cui, W., Cui, Y., Wang, J., Song, C., Mizokami, T. et al. (2006). Characterization of mesenchymal stem cells isolated from mouse fetal bone marrow. *Stem Cells* **24**, 482-493.
Watt, F. M. and Hogan, B. L. M. (2000). Out of Eden: stem cells and their niches. *Science* **287**, 1427-1430.
Wolber, F. M., Leonard, E., Michael, S., Orschell-Traycoff, C. M., Yoder, M. C. and Srour, E. F. (2002). Roles of spleen and liver in development of the murine hematopoietic system. *Exp. Hematol.* **30**, 1010-1019.
Wolf, N. S. and Trentin, J. J. (1968). Hemopoietic colony studies. V. Effect of hemopoietic organ stroma on differentiation of pluripotent stem cells. *J. Exp. Med.* **127**, 205-214.
Wu, H., Klingmüller, U., Acurio, A., Hsiao, J. G. and Lodish, H. F. (1997). Functional interaction of erythropoietin and stem cell factor receptors is essential for erythroid colony formation. *Proc. Natl. Acad. Sci. USA* **94**, 1806-1810.
Yanai, N., Matsuya, Y. and Obinata, M. (1989). Spleen stromal cell lines selectively support erythroid colony formation. *Blood* **74**, 2391-2397.
Zhang, C. C. and Lodish, H. F. (2004). Insulin-like growth factor 2 expressed in a novel fetal liver cell population is a growth factor for hematopoietic stem cells. *Blood* **103**, 2513-2521.
Zhang, C. C., Kaba, M., Ge, G., Xie, K., Tong, W., Hug, C. and Lodish, H. F. (2006). Angiopoietin-like proteins stimulate ex vivo expansion of hematopoietic stem cells. *Nat. Med.* **12**, 240-245.

Genes to Cells

Herbal drug ninjin'yoeito accelerates myelopoiesis but not erythropoiesis *in vitro*

Tomoko Inoue[1,2†], Kasem Kulkeaw[1†], Kanitta Muennu[1,3,4†], Yuka Tanaka[5,6], Yoichi Nakanishi[6] and Daisuke Sugiyama[1*]

[1]*Department of Research and Development of Next Generation Medicine, Faculty of Medical Sciences, Kyushu University, 3-1-1, Maidashi, Higashi-Ku, Fukuoka 812-8582, Japan*
[2]*Department of Medicine and Biosystemic Science, Graduate School of Medical Sciences, Kyushu University, 3-1-1, Maidashi, Higashi-Ku, Fukuoka 812-8582, Japan*
[3]*Thalassemia Research Center, Institute of Molecular Biosciences, Mahidol University, 25/25, Putthamonthon Sai 4 Rd. Salaya, Putthamonthon, 73170 Nakron Pratom, Thailand*
[4]*Faculty of Medical Technology, Prince of Songkla University, 15 Kanjanavanit Rd. Hat Yai, Songkhla, Thailand*
[5]*Department of Cell Biology, Faculty of Medicine, Fukuoka University, 7-45-1, Nanakuma, Jonan-ku, Fukuoka 814-0180, Japan*
[6]*Center for Clinical and Translational Research, Kyushu University Hospital, 3-1-1, Maidashi, Higashi-Ku, Fukuoka 812-8582, Japan*

Some Kampo medicines that are herbal and traditional in Japan have had beneficial effects when given to patients with anemia. However, molecular mechanisms underlying their effects are unclear. To address this question, four Kampo medicines used to treat anemia—ninjin'yoeito (NYT), shimotsuto (SMT), juzentaihoto (JTT), and daibofuto (DBT)—were tested separately using *in vitro* cultures of mouse bone marrow mononuclear cells. Among them, NYT was most effective in stimulating cell proliferation and up-regulating *Myc* expression. Flow cytometry analysis indicated that, among hematopoietic components of those cultures, myeloid cells expressing CD45/Mac-1/Gr-1/F4/80 increased in number, but Ter119/CD71 erythroid cells did not. Accordingly, real-time PCR analysis showed up-regulation of the myeloid gene *Pu.1*, whereas the erythroid genes *Gata1* and *Klf1* were down-regulated. Overall, these findings provide molecular evidence that NYT accelerates myelopoiesis but not erythropoiesis *in vitro*.

Introduction

Hematopoiesis is the process whereby functional, mature hematopoietic cells (red blood cells (RBCs), leukocytes, and platelets) are generated from hematopoietic stem cells in bone marrow (BM). Erythropoiesis is one aspect of hematopoiesis in which erythroid progenitors, such as burst forming unit-erythroid (BFU-E) and colony forming unit-erythroid (CFU-E) cells, are initially generated and then give rise to erythroblasts, reticulocytes, and finally RBCs, which contain hemoglobin functioning in oxygen transport (McGrath & Palis 2008). Failure of erythropoiesis results in a shortage of or damage to RBCs and underlies anemia.

Kampo is a Japanese herbal medicine and widely used to treat many kinds of diseases. Among them, the group shimotsuto, primarily in combination with other drugs, has been used clinically as a blood replenishment agent to treat anemia. Ninjin'yoeito (NYT), a member of shimotsuto group, reportedly antagonizes various forms of anemia, including iron-deficiency anemia (Yanagihori *et al.* 1995; Ando 1999), aplastic anemia (Ohmori *et al.* 1993; Miyazaki *et al.* 1994), refractory anemia (Ohmori *et al.* 1992; Nagoshi *et al.* 1993), renal anemia (Takemura 2000), and anemia resulting from anticancer therapies in humans (Motoo *et al.* 2005). In mice, oral administration of NYT improves 5-fluorouracil (5-FU) induced anemic conditions, as evidenced by the assessment of

Communicated by: Yo-ichi Nabeshima
**Correspondence:* ds-mons@yb3.so-net.ne.jp
†Equally contributed.

DOI: 10.1111/gtc.12143

reticulocyte and RBC numbers, hemoglobin and hematocrit levels in peripheral blood, and increases in BFU-E and CFU-E in BM (Takano *et al.* 2009). However, molecular mechanisms underlying NYT's effect have not been clarified in human beings or mice.

To address those mechanisms, we examined the effect of herbal remedies on cell proliferation and hematopoietic differentiation of BM mononuclear cells (MNCs) in mice by testing four Kampo medicines, NYT, SMT, JTT, and DBT, all historically used to treat anemia. We found that one of those, NYT, enhanced cell proliferation and up-regulated *Myc* transcript levels, likely accounting for the enhanced proliferative state. Among hematopoietic cells, NYT did not increase percentage of erythroid cells but rather decreased expression of the erythroid genes *Gata1* and *Klf1*, whereas the number of macrophages and granulocytes in cultures increased, accompanied by up-regulation of *Pu.1* expression.

Results

Hematopoietic cell proliferation in the presence of Kampo medicines

To investigate the effect of Kampo medicines on hematopoietic cell proliferation, we cultured BM MNCs separately with four Kampo medicines—ninjin'yoeito (NYT), daibofuto (DBT), juzentaihoto (JTT), or shimotsuto (SMT) (Table S1 and Fig. S1 in Supporting information)—for 11 days. To evaluate a potential direct effect of Kampo medicines, no cytokines were added to the cultures. Both round-shaped and adherent cells were observed in the negative control at day 11, while NYT treatment resulted in variable sizes of round-shaped cells and significant proliferation of the round cells by day 11 (Fig. 1A). Cells treated with SMT, JTT, or DBT exhibited similar morphological changes but showed fewer round-shaped cells (T. Inoue, K. Kulkeaw and K. Muennu, unpublished data). The total number of viable cells in negative control samples (♦) increased slightly by day 4 ($3.1 \pm 1.4 \times 10^5$ cells) and then decreased at days 8 and 11 ($0.5 \pm 0.03 \times 10^5$ and $0.76 \pm 0.1 \times 10^5$ cells, respectively). By contrast, BM MNCs cultured in the presence of NYT, SMT, or DBT exhibited significantly increased proliferation by day 11 ($P < 0.05$) (Fig. 1B). Specifically, NYT-treated cells (■) showed a slight increase at day 4 ($3.1 \pm 0.9 \times 10^5$ cells) and at day 8 ($3.5 \pm 2.1 \times 10^5$ cells) and then showed a 2.55-fold increase by day 11 ($8.9 \pm 3.3 \times 10^5$ cells). JTT-treated cells (●) showed the same trend: Their numbers were $2.6 \pm 1.0 \times 10^5$ cells at day 4, $2.8 \pm 1.8 \times 10^5$ at day 8, and $4.1 \pm 3.0 \times 10^5$ at day 11. However, compared with the negative control, no significant difference was observed in JTT-treated cells at day 11. By contrast, DBT-treated cells (**x**) decreased in number by day 4 ($2.1 \pm 0.6 \times 10^5$ cells) but then consistently increased at days 8 ($4.5 \pm 2.5 \times 10^5$ cells) and 11 ($5.7 \pm 2.0 \times 10^5$ cells). SMT-treated cells (▲) showed the same trend as DBT-treated cells: Their numbers were $2.4 \pm 0.5 \times 10^5$ at day 4, $3.5 \pm 2.9 \times 10^5$ at day 8, and $4.9 \pm 1.1 \times 10^5$ at day 11 (Fig. 1B).

To assess molecular mechanisms underlying cell proliferation, we used real-time PCR to examine expression of the transcription factor *Myc*, which functions in cell proliferation (Fig. 1C). Regardless of the type of Kampo medicine used, *Myc* expression in cell cultures gradually increased, including that seen in the negative control. DBT- and JTT-treated cultures showed lower *Myc* expression than did the negative control, whereas NYT-treated cells showed the highest *Myc* expression (day 4: 0.52 ± 0.03, day 8: 0.70 ± 0.01 and day 11: 1.64 ± 0.21) among all culture conditions at all time points (Fig. 1C). Particularly at day 11, *Myc* expression in NYT-treated cells increased significantly relative to the negative control (1.64 ± 0.21 versus 0.49 ± 0.12; $P = 0.02$) (Fig. 1C).

NYT consists of 12 component medical plants, such as Japanese Angelica root, Rehmannia root, peony root, atractylodes rhizome, Poroa Sclerotium, ginseng, cinnamon bark, Polygala root, Citrus unshiu peel, Astragalus root, Glycyrrhiza and Schisandra fruit. To determine whether the herbal constituents of NYT act synergistically to stimulate cell proliferation, cultures were treated with individual NYT components and assessed for cell number and *Myc* expression. As shown in Fig. S2 and Fig. 1D, all NYT components except for Poria sclerotium and cinnamon bark enhanced proliferation relative to controls. *Myc* expression increased in the presence of Japanese Angelica root ($P = 0.0005$) and Rehmannia root ($P = 0.0002$) but remained lower than that stimulated by NYT (Fig. 1E), suggesting that NYT components act synergistically and that Japanese Angelica root and Rehmannia root are likely essential NYT components.

NYT does not alter erythropoiesis in bone marrow mononuclear cells

We next examined the effect of NYT on erythroid cell differentiation. Both $CD71^+/Ter119^+$ cells

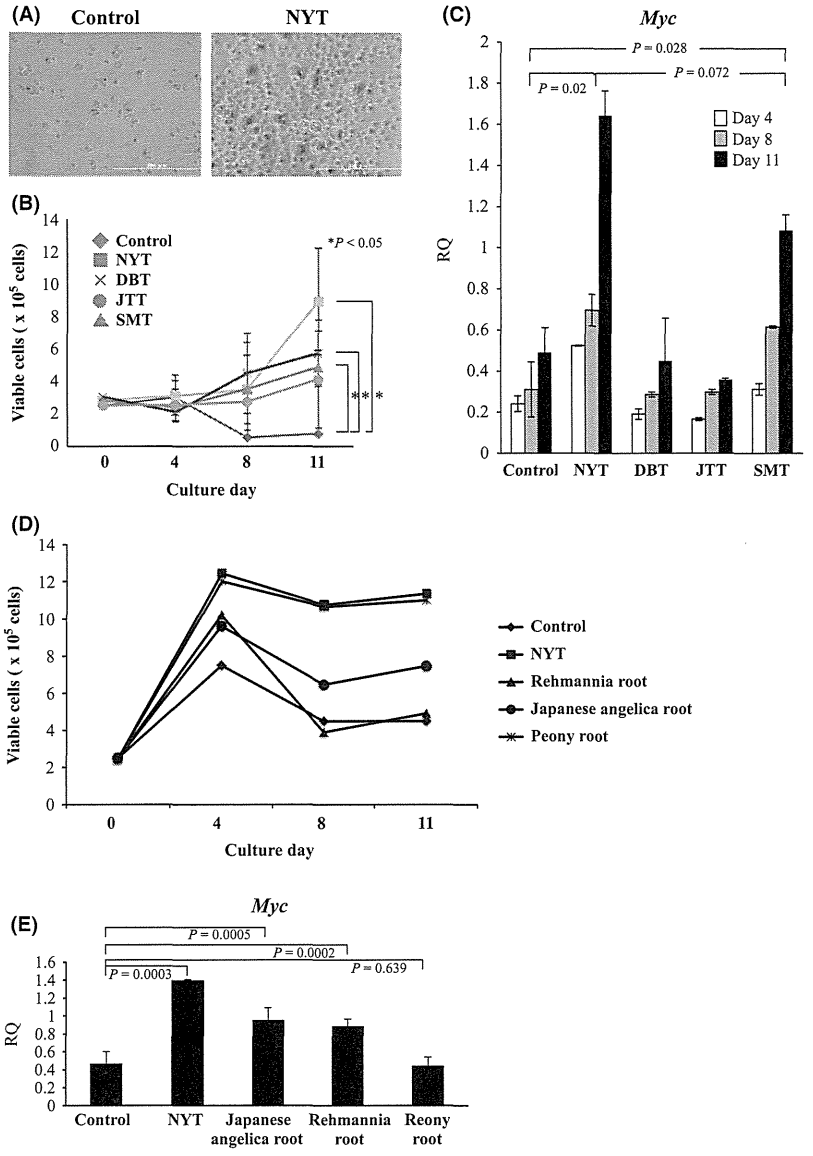

Figure 1 Hematopoietic cell proliferation in the presence of Kampo medicines. (A) Morphology of cells derived from cultured BM MNCs after 11 days of NYT treatment. Shown are phase-contrast images. Scale bars: 200 μm. (B) Total number of viable cells after Kampo medicine treatment. BM MNCs were collected, and viable cells were counted using trypan blue dye after 4, 8, and 11 days. (C), (E) Quantitative real-time PCR analysis of the cell proliferation marker *Myc* at days 4, 8, and 11 (day 11 in E) of cultured BM MNCs. Data are normalized to β-*actin* expression. Student's *t*-test * was used to calculate statistical significant difference ($P < 0.05$). (D) Total number of viable cells after treatment of NYT and components (Rehmannia root, Japanese Angelica root and Peony root). BM MNCs were collected, and viable cells were counted using trypan blue dye after 4, 8, and 11 days.

representing erythroblasts and $CD71^-/Ter119^+$ cells representing mature erythrocytes were analyzed at days 4, 8, and 11 by flow cytometry. $CD71^-/Ter119^+$ erythrocytes were generated at low efficiency (< 0.6%) in cell culture (Fig. 2A). A significant decrease in the number of $Ter119^+$ cells in NYT-treated culture (1.5 times lower) was observed at day 8, whereas there was no significant difference between $CD71^-/Ter119^+$ cells at days 4 and 11 (Fig. 2B). In agreement, real-time PCR analysis showed that expression of the erythropoietic transcription factor *Gata1* (Whitelaw *et al.* 1990) was

higher in control versus NYT-treated cells (day 4: 0.8 ± 0.16 in controls and 0.147 ± 0.09 in NYT-treated cells; and day 8: 0.419 ± 0.07 in controls and no expression in NYT-treated cells) (Fig. 2C). The transcription factor *Klf1* (Miller & Bieker 1993), whose expression is regulated by Gata1, was detected in controls and NYT-treated cells only on day 4 but not days 8 and 11. No expression of *Klf1* was seen after SMT, JTT, or DBT treatment (T. Inoue, K. Kulkeaw and K. Muennu, unpublished data). These findings indicate that NYT does not accelerate erythroid differentiation.

NYT accelerates myelopoiesis of bone marrow mononuclear cells

To investigate the effect of NYT on leukopoiesis, which consists of myelopoiesis and lymphopoiesis, we examined expression of the common leukocyte antigen CD45, a pan-leukocyte marker, at days 4, 8 (T. Inoue, K. Kulkeaw and K. Muennu, unpublished data), and 11 (Fig. S3A, left in Supporting information) by flow cytometry. Percentage of $CD45^+$ cell was slightly higher in NYT-treated cells (control: 95.1 ± 1.33%, NYT-treated cells: 97.6 ± 0.28%), but the difference was not statistically significant ($P = 0.118$) (Fig. S3A in Supporting information). When leukopoiesis was analyzed by flow cytometry using Mac-1 (CD11b), a marker of macrophages and granulocytes, and B220, a B-lymphocyte marker, NYT-treated BM MNCs differentiated into $CD45^+$/$Mac\text{-}1^+$ cells in numbers 2.23 times greater than controls ($P = 0.002$) (Fig. S3B in Supporting information) and into $CD45^+/Mac\text{-}1^-/B220^+$ B lymphocytes in numbers 3.00 times lower than control ($P = 0.002$) (Fig. S3B in Supporting information) by 11 days in culture. In agreement with the increase in $CD45^+/Mac\text{-}1^+$ cells, real-time PCR analysis showed that expression of *Pu.1 (Spi1)*, which positively regulates generation of macrophages and granulocytes, was higher in NYT-treated cells (1.00 ± 0.001 in controls and 5.55 ± 0.09 in NYT-treated cells) ($P = 0.007$) (Fig. S3C in Supporting information). Also, expression of colony-stimulating factor 1 receptor (*Csf1r*), the receptor for macrophage colony-stimulating factor, was higher in NYT-treated (1.12 ± 0.09 in controls and 1.53 ± 0.08 in NYT-treated cells) ($P = 0.06$) at day 11 (Fig. S3C in Supporting information). Taken together, these findings suggest that the primary effect of NYT on hematopoiesis is to accelerate myelopoiesis.

To investigate NYT activity using purified populations, we removed erythroid cells by sorting $CD45^+$/$Ter119^-$ cells from BM MNCs (Fig. 3A) and then

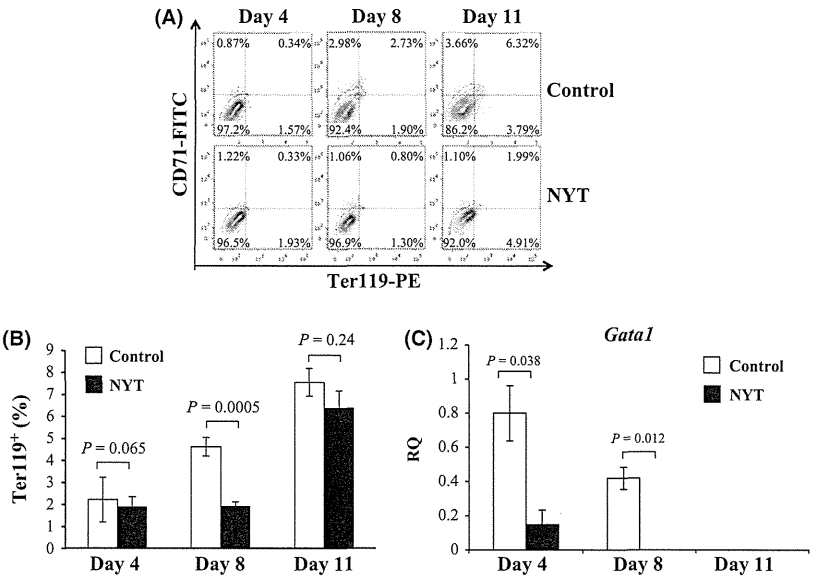

Figure 2 NYT treatment does not alter erythropoiesis. (A) BM MNCs cultured with and without NYT were collected at days 4, 8, and 11, and erythroid differentiation was assessed by flow cytometric analysis of cells stained positive for CD71 and Ter119. The percentage of $Ter119^+$ erythroid cells is shown in (B). (C) Quantitative real-time PCR analysis of the erythroid gene *Gata1* at days 4, 8, and 11. Data were assessed by normalized values to control at day 4.

cultured them in the presence of NYT for 11 days. The total number of cells in the untreated negative control group increased at day 4 ($2.93 \pm 0.11 \times 10^5$ cells) and then decreased at days 8 and 11 ($2.40 \pm 0.84 \times 10^5$ and $2.10 \pm 0.42 \times 10^5$ cells, respectively). By contrast, NYT-treated $CD45^+$ cells showed a 2.4-fold increase in total cell number at day 4 ($4.80 \pm 0.21 \times 10^5$ cells) ($P = 0.007$), decreased at day 8 ($4.20 \pm 0.42 \times 10^5$ cells) ($P = 0.116$), and then increased at day 11 ($6.75 \pm 1.06 \times 10^5$ cells) ($P = 0.029$) (Fig. 3B). Flow cytometric analysis (Fig. 3C) showed that $CD45^+$ cells were more abundant in NYT-treated ($94.0 \pm 0.46\%$) versus control ($73.7 \pm 1.89\%$) cells ($P = 0.0001$) (Fig. 3C). Among $CD45^+$ cells, the proportion of $Mac\text{-}1^+/F4/80^+$ macrophages differentiated from BM MNC $CD45^+$ cells was 8.05 times higher in NYT-treated than in control cells ($P = 0.01$) (Fig. 3D). Moreover, the proportion of $Mac\text{-}1^+/Gr\text{-}1^+$ granulocytes was 3.41 times higher in NYT-treated than control cells ($P = 7.07 \times 10^{-6}$) (Fig. 3E). Furthermore, real-time PCR analysis showed that expression of *Pu.1* was higher in cultures of NYT-treated compared with control cells (3.15-fold at day 4, 1.28-fold at day 8 and 5.43-fold at day 11) (Fig. 3F). *Csf1r* expression was 8.41 times lower in NYT-treated compared with control cells at day 4, 4.72 times higher at day 8, and 2.66 times higher at day 11 (Fig. 3F).

To determine which stage of myeloid differentiation is affected by NYT, we carried out CFU assays. No colonies were produced without addition of cytokines (T. Inoue, K. Kulkeaw and K. Muennu, unpublished data). In the presence of the myeloid cytokines SCF, IL-3, and IL-6, NYT increased total colony number 1.30-fold ($P = 0.528$). Among those colonies, the number of CFU-M, CFU-G, and CFU-GM, all indicative of committed myeloid progenitors, increased, implying that NYT accelerates myelopoiesis at the progenitor level (Fig. S4 in Supporting information).

Gene expression changes in bone marrow cells

To identify hematopoietic genes regulated by NYT, microarray analysis was carried out to compare BM MNCs cultured with and without NYT for 11 days. Up-regulated ($P < 0.05$) and down-regulated ($P < 0.05$) genes were analyzed and categorized functionally (Fig. S5 in Supporting information). In agreement with results shown in Fig. 3F and Fig. S4, we identified factors affecting leukopoiesis. Among them, we observed down-regulation of *Rasgrp1* (de la Luz Sierra *et al.* 2010) and *Dok2* (Garcia *et al.* 2004) after 11 days in culture with NYT (7.31-fold decrease ($P = 0.0005$) and 1.78-fold decrease ($P = 0.003$), respectively) (Fig. 3G), a finding validated by real-time PCR.

Discussion

Here, we assessed molecular mechanisms underlying the effect of Kampo medicines on erythropoiesis. Among four such medicines tested, NYT showed the greatest stimulation of BM MNC proliferation accompanied by the highest up-regulation of *Myc*, a factor associated with up-regulated proliferation, by 11 days after culture (Fig 1B). Relevant to proliferation, our findings are in accordance with a report that NYT increased the number of primary rat oligodendrocyte precursors *in vitro* as assessed by BrdU incorporation studies (Kobayashi *et al.* 2003).

Previously, others had shown that after induction of anemia, NYT stimulates erythroid cell differentiation (Takatsuki *et al.* 1996; Takano *et al.* 2009). Thus, we initially hypothesized that Kampo medicines would accelerate erythropoiesis. However, in our cul-

Figure 3 Effect of NYT on myeloid differentiation of BM $CD45^+$ cells. (A) $CD45^+/Ter119^-$ leukocytes were isolated from BM MNCs to remove erythroid cells and cultured for 11 days. (B) Viable cells were collected at days 4, 8, and 11 and counted using trypan blue dye. (C) BM $CD45^+$ leukocytes cultured with and without NYT were collected at day 11, and leukocyte differentiation was assessed by flow cytometry based on CD45 staining. The percentage of $CD45^+$ leukocytes is shown at right. (D) Myeloid differentiation of $CD45^+$ cells was evaluated by flow cytometry at day 11 based on staining with Mac-1 (CD11b) and F4/80. The percentage of $CD45^+/Mac\text{-}1^+/F4/80^+$ macrophages is shown at right. (E) Granulocyte differentiation of $CD45^+$ cells was evaluated by flow cytometry at day 11 based on staining with Mac-1 (CD11b) and Gr-1. The percentage of $CD45^+/Mac\text{-}1^+/Gr\text{-}1^+$ granulocytes is shown at right. (F) Quantitative real-time PCR analysis of expression of the myeloid genes *Pu.1* and *Csf1r* at days 4, 8, and 11. Data were assessed by normalized values to control at day 4. (G) BM MNCs cultured with and without NYT *in vitro* were collected and analyzed by quantitative real-time PCR at day 11 for expression of *Rasgrp1*, a lymphopoietic gene, and *Dok2*, a myelopoietic gene. Data are normalized to β-*actin* expression.

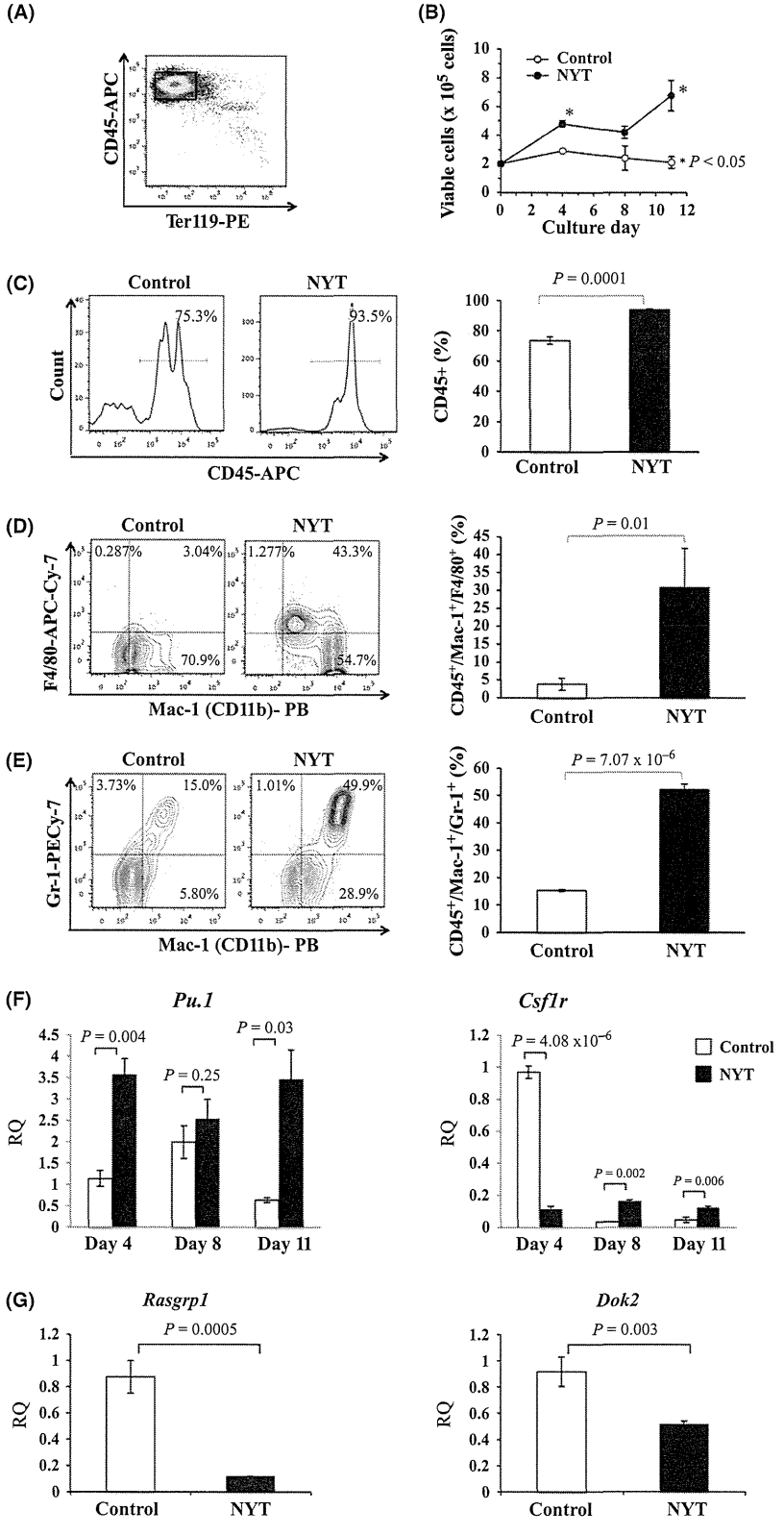

ture conditions, we did not observe up-regulation of *Gata1* and *Klf1* mRNAs or of Ter119 proteins—markers of erythropoiesis—after NYT treatment (Fig. S3 in Supporting information). These discrepancies suggest that NYT activity may differ in normal homeostasis compared with anemic conditions. However, when we evaluated leukopoiesis, we found that culturing BM MNCs for 11 days in NYT accelerated myelopoiesis but not lymphopoiesis, based on flow cytometric and gene expression analysis (Fig. S3B in Supporting information). Previously, Okamura *et al.* reported that NYT dose dependently augmented production of GM-CSF but not G-CSF, as evaluated by ELISA analysis of human peripheral blood MNCs after 3 days of culture (Okamura *et al.* 1991). However, we did not observe expression of *GM-CSF* and *G-CSF* transcripts at days 4, 8, or 11 in $CD45^+$ cells derived from BM MNCs cultured with NYT (T. Inoue, K. Kulkeaw and K. Muennu, unpublished data). These discrepancies may be attributable to species differences or culture conditions. Miura *et al.* reported that intraperitoneal NYT administration in mice increased the number of macrophages in both the peritoneal cavity and spleen within 7 to 10 days (Miura *et al.* 1989).

Some bioactive ingredients of JTT, such as polysaccharides and fatty acids, reportedly have proliferative effect on hematopoietic cells. Polysaccharides obtained from Glycyrrhiza, a component of JTT exhibited mitogenic activity that influences the selective proliferation of B cells (Yamada & Saiki 2005). Fatty acids, such as oleic and linoleic acids, stimulate the proliferation of hematopoietic stem cells *in vitro* (Hisha *et al.* 1997). As Kampo medicines tested in this study originally include polysaccharides and fatty acids, we cannot deny the possibility that these bioactive ingredients of NYT might affect the myeloid cell proliferation from BM MNCs (Fig. 1B). It will be a topic in the future.

In summary, we provide the molecular evidence that NYT accelerates myelopoiesis *in vitro*.

Experimental procedures

Mice

C57BL/6 (2–4 months) mice were purchased from Nihon SLC (Hamamatsu, Japan) and Kyudo (Tosu, Japan). Animals were handled according to the Guidelines for Laboratory Animals of Kyushu University. This study was approved by the Animal Care and Use Committee, Kyushu University (Approval ID: A21-068-0).

Preparation of Kampo medicines

Kampo medicines including NYT, SMT, JTT, and DBT (Table S1 and Fig. S1 in Supporting information) (Tsumura & Co, Tokyo, Japan) were freshly prepared as follows. First, 0.25 g of each Kampo medicine extract powder was dissolved in 5 mL of hot distilled water (at a final concentration of 50 mg/mL). The solution was centrifuged at 2395 ***g*** for 10 min, and supernatants were filtered through 0.45-μm filters.

Primary cell culture

BM cells were harvested by flushing femurs of 2–4 months C57BL/6 mice with Iscove's Modified Dulbecco's Medium (IMDM, SIGMA-ALDRICH, St. Louis, MO) supplemented with 2% fetal bovine serum (FBS). After one PBS wash, cells were incubated with red blood cell lysis buffer (0.16 M NH_3Cl, 10 mM $KHCO_3$, 5 mM EDTA) on ice for 10 min, and then mononuclear cells (MNCs) were separated using Lympholyte-M (Density: 1.0875 + 0.0010 g/cm^3, CEDARLANE®) according to the manufacturer's instruction. BM MNCs were cultured with IMDM containing 10 μg/mL Kampo supernatant, 15% FBS, 0.1% 2-mercaptoethanol, and 10 U/mL penicillin/10 μg/mL streptomycin (SIGMA-ALDRICH). Negative controls were cultured in the same media without Kampo medicines. Cells were incubated at 37 °C, 5% CO_2, and 95% humidity. Culture media were changed at day 8. Cells were collected for counting and analysis at days 4, 8, and 11 of culture. The number of viable cells was determined using trypan blue staining. To assess the effect of Kampo medicines on $CD45^+$ leukocytes, BM MNCs were stained with anti-CD45-APC antibody (Ab) (eBioscience, San Diego, CA) and sorted using a FACS Aria cell sorter (BDIS, San Jose, CA). $CD45^+$ cells were cultured with respective Kampo medicines and noncytokine-containing medium according to methods described above.

Quantitative real-time PCR

Total RNA was extracted from cultures of BM MNCs and $CD45^+$ cells using a RiboPure™ Kit (Life Technologies, Carlsbad, CA). Total RNA was subjected to reverse transcription using a High-Capacity RNA-to-cDNA Kit (Life Technologies) according to established protocols. Gene expression levels were measured by StepOnePlus™ Real-Time PCR (Life Technologies) with TaqMan® Gene Expression Master Mix. All probes (*Myc, Gata1, Pu.1, Csf1r, Rasgrp1* and *Dok2*) were from TaqMan® Gene Expression Assays. PCR conditions were as follows: denaturation at 95 °C for 10 s, annealing at 60 °C for 20 s (40 cycles), and extension at 72 °C for 20 s. A final dissociation stage was carried out consisting of 95 °C for 15 s, 60 °C for 1 min, and 95 °C for 15 s. β-*actin* served as internal control. Normalized values ($-2^{\Delta\Delta C_t}$, ddCT) were compared among samples, and experiments were carried out in triplicate.

Microarray analysis

BM MNCs cultured with NYT or negative controls were collected at day 11. Total RNA was extracted using RNeasy® Plus Micro Kit (QIAGEN). RNA concentration was measured by NANODROP 2000c (Thermo Fisher Scientific). cRNA was amplified, labeled, and hybridized to an Agilent Whole Mouse GE 4 × 44K v2 Microarray (Agilent Technologies, Santa Clara, CA, USA) according to the manufacturer's instructions. All hybridized microarrays were scanned using an Agilent scanner, and signals of all probes were analyzed using Feature Extraction Software (9.5.1.1) (Agilent Technologies).

Flow cytometry

To analyze erythroid differentiation, cells were stained with anti-Ter119-PE Ab and anti-CD71-FITC Ab (BD Bioscience). To analyze myeloid and lymphoid differentiation, cells were stained with anti-Mac-1-PB Ab (Biolegend, San Diego, CA) and anti-B220-APC-Cy7 Ab (Biolegend). To isolate $CD45^+Ter119^-$ cells, BM MNCs were stained with anti-CD45-APC Ab (Biolegend) and anti-Ter119-PE Ab. To identify leukocytes, $CD45^+$ cultured cells were stained with anti-Mac-1-PB Ab, anti-F4/80-APC-Cy7 Ab (Biolegend) and anti-Gr-1-PE-Cy7 Ab (Biolegend).

Colony formation assay

BM MNCs were suspended in 4 mL of MethoCult® GF M3234 (Stemcell Technologies) supplemented with IL-3 (10 ng/mL), IL-6 (10 ng/mL), and SCF (50 ng/mL) and distributed into three 35-mm dishes (1×10^4 cells/dish). Cells were then incubated with 5% CO_2 at 37 °C. Colonies were counted on days 10–12 using an inverted phase-contrast microscope CKX41 (Olympus, Tokyo, Japan).

Statistical analysis

Data are presented as means plus standard deviation (SD). Student's *t*-test was used to calculate statistical significance. A *P*-value <0.05 was considered statistically significance.

Acknowledgements

This work was supported by a grant from the Ministry of Health, Labour and Walfare, Japan and by a bilateral program between Japan and Thailand, which are supported by the Japan Society for the Promotion of Science (JSPS) and National Research Council of Thailand (NRCT). T. Inoue and K. Kulkeaw were supported by postdoctoral fellowships for Young Scientists from the JSPS. K. Muennu was supported by a postdoctoral fellowship from Mahidol University, the Heiwa Nakajima Foundation and Prince of Songkla University. The authors would like to thank Drs. F. Suthat, S. Saovaros, K. Akashi for helpful discussion, and Dr. Elise Lamar for critical reading of the manuscript.

References

Ando, N. (1999) Blood making effect of Ninjin-yoei-to (Ren-shen-yang-rong-tang) as monotherapy in obesteric and gynecologic patient with anemia. *Jpn. J. Orient. Med.* **50**, 461–470.

Garcia, A., Prabhakar, S., Hughan, S., Anderson, T.W., Brock, C.J., Pearce, A.C., Dwek, R.A., Watson, S.P., Hebestreit, H.F. & Zitzmann, N. (2004) Differential proteome analysis of TRAP-activated platelets: involvement of DOK-2 and phosphorylation of RGS proteins. *Blood* **103**, 2088–2095.

Hisha, H., Yamada, H., Sakurai, M.H., Kiyohara, H., Li, Y., Yu, C., Takemoto, N., Kawamura, H., Yamamura, K., Shinohara, S., Komatsu, Y., Aburada, M. & Ikehara, S. (1997) Isolation and identification of hematopoietic stem cell-stimulating substances from Kampo (Japanese herbal) medicine, Juzen-taiho-to. *Blood* **90**, 1022–1030.

Kobayashi, J., Seiwa, C., Sakai, T., Gotoh, M., Komatsu, Y., Yamamoto, M., Fukutake, M., Matsuno, K., Sakurai, Y., Kawano, Y. & Asou, H. (2003) Effect of a traditional Chinese herbal medicine, Ren-Shen-Yang-Rong-Tang (Japanese name: Ninjin-Youei-To), on oligodendrocyte precursor cells from aged-rat brain. *Int. Immunopharmacol.* **3**, 1027–1039.

de la Luz Sierra, M., Sakakibara, S., Gasperini, P., Salvucci, O., Jiang, K., McCormick, P.J., Segarra, M., Stone, J., Maric, D., Zhu, J., Qian, X., Lowy, D.R. & Tosato, G. (2010) The transcription factor Gfi1 regulates G-CSF signaling and neutrophil development through the Ras activator RasGRP1. *Blood* **115**, 3970–3979.

McGrath, K. & Palis, J. (2008) Ontogeny of erythropoiesis in the mammalian embryo. *Curr. Top. Dev. Biol.* **82**, 1–22.

Miller, I.J. & Bieker, J.J. (1993) A novel, erythroid cell-specific murine transcription factor that binds to the CACCC element and is related to the Kruppel family of nuclear proteins. *Mol. Cell. Biol.* **13**, 2776–2786.

Miura, S., Kawamura, I., Yamada, A., Kawakita, T., Kumazawa, Y., Himeno, K. & Nomoto, K. (1989) Effect of a traditional Chinese herbal medicine ren-shen-yang-rong-tang (Japanese name: ninjin-youei-to) on hematopoietic stem cells in mice. *Int. J. Immunopharmacol.* **11**, 771–780.

Miyazaki, T., Uchini, H., Kimura, I., Saito, H., Shibaa, A., Takaku, F., Niho, Y., Matsuda, T., Miura, A., Imamura, M., Kitamura, K. & Hotta, T. (1994) Effects of Ren-shen-yang-rong-tang (Japanese name: Ninjin-youei-to), a traditional herbal medicine, on the hematopoiesis in the patients with aplastic anemia. *Rinsyou Iyaku* **10**, 189–201.

Motoo, Y., Mouri, H., Ohtsubo, K., Yamaguchi, Y., Watanabe, H. & Sawabu, N. (2005) Herbal medicine Ninjinyoeito ameliorates ribavirin-induced anemia in chronic hepatitis C: a randomized controlled trial. *World J. Gastroenterol.* **11**, 4013–4017.

Nagoshi, H., Irako, A., Takahashi, A., Fukumura, R., Nomura, M., Takahashi, S., Isobe, H., Ide, K. & Someya, K. (1993) Clinical effect of Ren-Shen-Yang-Rong-Tang (Japanese

Name: Ninjin-Yoei-To) on refractory anemia in the Elderly. *Jpn Pharmacol. Ther.* **21**, 4789–4795.

Ohmori, M., Suzuki, T., Omori, S. & Yasuda, N. (1993) A case of aplastic anemia-PNH syndrome treated with a traditional chinese herbal medicine, EK-108. *Jpn Pharmacol. Ther.* **21**, 553–556.

Ohmori, S., Usui, T., Yasuda, N., Ohmori, M., Yamagishi, M. & Okuma, M. (1992) Improvement of anemia by administration of EK-108 [Chinese herbal medicine, Ren-Shen-Yang-Rong-Tang (Japanese name, Ninjin-Yoei-To)] in a patient of myelodisplastic syndrome. *Jpn Pharmacol. Ther.* **20**, 361–365.

Okamura, S., Shimoda, K., Yu, L.X., Omori, F. & Niho, Y. (1991) A traditional Chinese herbal medicine, ren-shen-yang-rong-tang (Japanese name: ninjin-yoei-to) augments the production of granulocyte-macrophage colony-stimulating factor from human peripheral blood mononuclear cells in vitro. *Int. J. Immunopharmacol.* **13**, 595–598.

Takano, F., Ohta, Y., Tanaka, T., Sasaki, K., Kobayashi, K., Takahashi, T., Yahagi, N., Yoshizaki, F., Fushiya, S. & Ohta, T. (2009) Oral Administration of Ren-Shen-Yang-Rong-Tang 'Ninjin'yoeito' Protects Against Hematotoxicity and Induces Immature Erythroid Progenitor Cells in 5-Fluorouracil-induced Anemia. *Evid. Based Complement. Alternat. Med.* **6**, 247–256.

Takatsuki, F., Miyasaka, Y., Kikuchi, T., Suzuki, M. & Hamuro, J. (1996) Improvement of erythroid toxicity by lentinan and erythropoietin in mice treated with chemotherapeutic agents. *Exp. Hematol.* **24**, 416–422.

Takemura, K. (2000) Effect of Ninjin-Youeitoh on renal anemia in hemodialysis patients treated by recombinant human erythropoietin. *Kampo to Saishintiryou* **9**, 271–274.

Whitelaw, E., Tsai, S.F., Hogben, P. & Orkin, S.H. (1990) Regulated expression of globin chains and the erythroid transcription factor GATA-1 during erythropoiesis in the developing mouse. *Mol. Cell. Biol.* **10**, 6596–6606.

Yamada, H. & Saiki, I. (2005) *Juzen-taiho-to (Shi-Quan-Da-Bu-Tang): Scientific Evaluation and Clinical Applications*. Boca Raton, FL: CRC Press.

Yanagihori, A., Miyagi, M., Hori, M., Ohtaka, K., Matsushima, H. & Itoh, M. (1995) Effect of Ninjin-Yoei-To on iron-deficiency anemia. *Rinsyou to Kenkyu* **72**, 231–234.

Received: 18 November 2013
Accepted: 29 January 2014

Supporting Information

Additional Supporting Information may be found in the online version of this article at the publisher's web site:

Figure S1 3D HPLC pattern of Kampo medicines.

Figure S2 Hematopoietic cell proliferation in the presence of NYT and its components.

Figure S3 Effect of NYT on leukopoiesis of BM MNCs.

Figure S4 NYT accelerates hematopoietic colony formation.

Figure S5 Global changes in gene expression observed in NYT-treated BM cells.

Table S1 Components of four Kampo medicines

ANTICANCER RESEARCH *34*: 4539-4550 (2014)

Multicolor Analysis of Cell Surface Marker of Human Leukemia Cell Lines Using Flow Cytometry

TOMOKO INOUE[1], ANTHONY SWAIN[1], YOICHI NAKANISHI[2] and DAISUKE SUGIYAMA[1]

[1]*Department of Research and Development of Next-Generation Medicine, Faculty of Medical Sciences, Kyushu University, Fukuoka, Japan;*
[2]*Center for Clinical and Translational Research, Kyushu University Hospital, Fukuoka, Japan*

Abstract. *Background: Leukemia cell lines are utilized as tools for molecular analysis. Their implementation in therapy will require standards for quality control, including appropriate selection criteria for functional analysis and efficacy determination. Materials and Methods: Characteristics of six human leukemia cell lines –Kasumi-1, NB-4, MOLM-13, MV-4-11, K562, and Jurkat cells– were investigated using multiple color analysis of surface antigen expression and comparative analysis of gene expression. Results: Differentiation states of Kasumi-1 and MOLM-13 cells are colony-forming units-granulocyte/macrophage equivalent cells to myeloblasts with comparatively high Growth factor independent-1(GFI1) and Transcription factor PU.1 (PU.1) expression, respectively. NB4 and MV-4-11 express high levels of CCAAT/enhancer-binding protein-alpha (CEBPα) and differentiate from myeloblasts to pro-monocytes and myeloblasts, respectively. K562 cells are colony-forming units-erythroid equivalent cells to erythroblasts, with the highest expression of GATA-binding factor 2 (GATA2), GATA1 and Friend of gata-1 (FOG1). Jurkat cells are pro-T to mature T-cells with the highest Neurogenic locus notch-1 homolog protein 1 (NOTCH1) expression. Conclusion: Our study gives a useful guideline of standards for appropriate usage of leukemia cell lines for examining novel targets in vitro.*

Leukemias are a group of disorders characterized by abnormal growth and differentiation of hematopoietic cells due to several factors, including chromosomal abnormalities and transcription factor alterations, which lead to anemia, neutropenia and thrombocytopenia. In almost all cases, leukemia is classified as one of four types; acute myelogenous leukemia (AML), acute lymphocytic leukemia (ALL), chronic myelogenous leukemia (CML), and chronic lymphocytic leukemia (CLL). In acute leukemia, leukocytes proliferate rapidly in the bone marrow at an immature state, and therefore cannot function normally. On the other hand, in chronic leukemia, blastic cells form more slowly than in acute leukemia and consequently cells with abnormal function are transported to the hematopoietic tissues. In AML and CML, myeloid lineage cells such as granulocytes and monocytes, become malignant and lose the capacity to differentiate into mature functional cells and interfere with the production of normal blood cells. In ALL and CLL, lymphoid lineage cells such as T- and B-lymphocytes do likewise. There is considerable research taking place utilizing leukemia cells (both primary cells and immortalized cell lines) to elucidate their pathogenetic mechanisms at cellular and molecular levels, and to develop novel therapies (for example, gene therapy and molecular-target therapy) in addition to existing therapeutic methods, such as chemotherapy, hematopoietic stem cell transplantation, transfusion therapy and induction therapy.

Primary cells from patients with leukemia are obtained from peripheral blood (PB) and bone marrow (BM), which provide much information for diagnosis through morphological observation, cell surface antigen-dependent phenotypical observations and chromosomal tests. However, as primary cells are limited in number and accessibility (especially for BM), it is not easy to extract them for functional analysis in order to examine novel targets to treat patients. To overcome this problem, immortalized leukemia cell lines that can proliferate indefinitely were established and are being utilized as useful tools to analyze molecular mechanisms (transcription factors, signaling pathways, translocations) (1, 2). They are also used for analysis of both gain-of-function, with plasmid transfection and use of recombinant protein, and loss-of-function, with siRNA/shRNA transfection and inhibitors (3, 4).

Correspondence to: Dr. Tomoko Inoue and Dr. Daisuke Sugiyama, Department of Research and Development of Next-Generation Medicine, Faculty of Medical Sciences, Kyushu University, 3-1-1, Maidashi, Higashi-Ku, Fukuoka, 812-8582, Japan. Tel: +81 926426210, Fax: +81 926426146, e-mail: yokotomo@hsc.med.kyushu-u.ac.jp (Tomoko Inoue), ds-mons@yb3.so-net.ne.jp (Daisuke Sugiyama)

Key Words: Leukemia cell line, cell surface marker, flow cytometry.

When the cell lines were established, expressions of cell surface markers were studied in terms of single antigens but not multiple antigens together. The transcription factors were examined individually and not compared to other cell lines. It is necessary to characterize leukemia cell lines in terms of protein and gene expression levels, so as to evaluate the state of differentiation and maturation more precisely, which will be very useful in controlling the quality of cell lines, as well as in choosing cell lines to evaluate the effects of molecules and therapies.

Multi-parametric flow cytometry is an adequate method for gaining information on the cell differentiation state, monitoring residual disease and evaluating response to therapy (5, 6). Such application of flow cytometry has become more widespread, and will require the development of standardized approaches with defined specificity and sensitivity, along with suitable quality control schemes.

Herein we examined the multiple color analysis of cell surface markers and comparative analysis of transcription gene expression in using six human leukemia cell lines: four myeloblastic and monoblastic leukemia cell lines: Kasumi-1 (7), NB-4 (8), MOLM-13 (9) and MV-4-11 (10); an erythroleukemia cell line, K562 (11); and the T-cell leukemic cell line Jurkat (12), which have been previously used as *in vitro* leukemia models.

Materials and Methods

Cell culture. The human leukemia cell lines, Kasumi-1, NB4, MOLM-13, K562 and Jurkat were cultured in RPMI-1640 medium (Wako Pure Chemical Industries, Osaka, Japan) supplemented with 10% fetal bovine serum and MV-4-11 cells were cultured in RPMI-1640 medium supplemented with 10% fetal bovine serum and 10 ng/ml human recombinant Granulocyte/macrophage colony-stimulating factor (GM-CSF) (PeproTech, Rochy Hill, NJ, USA) at 37°C in 5% CO_2.

Cell morphology. Slides of cell suspensions were prepared by CytoSpin 4 (Thermo Fisher scientific, Waltham, MA, USA) at 450 rpm (rcf, 26.06 × *g*) for 7 minutes. Cells were stained with May-Grunwald and Giemsa staining reagents (Muto Pure Chemicals, Tokyo, Japan) and characterized morphologically. One slide containing 2×10^4 cells was prepared for each cell line. Stained cells were observed using an Olympus CKX41 microscope (Olympus, Tokyo, Japan).

Flow cytometry. Kasumi-1 cells and NB4 cells: To analyze hematopoietic stem/progenitor cell (HSPC) markers, cells were stained with a Fluorescein isothiocyanate (FITC)-conjugated anti-human Cluster of differentiation (CD)38 (Biolegend, San Diego, CA, USA), Phycoerythrin (PE)-Cy7-conjugated anti-human Tyrosine-protein kinase (c-KIT, CD117) (Biolegend), Allophycocyanin (APC)-conjugated anti-human CD34 (eBioscience, San Diego, CA, USA), APC-Cy7-conjugated anti-human CD13 (Biolegend) and Pacific Blue-conjugated anti-human leukocyte antigen (HLA)-DR (Biolegend). In addition, PE-conjugated anti-human CD135 (Biolegend) for Kasumi cells and PE-conjugated anti-human CD33 (Biolegend) for NB4 cells were stained to analyze the cells.

To analyze myeloid cell lineage markers, cells were stained with a FITC-conjugated anti-human CD15 (Biolegend), PE-conjugated anti-human CD116 (Biolegend), PE-Cy7-conjugated anti-human CD14 (Biolegend), APC-conjugated anti-human CD11c (Biolegend), APC-Cy7-conjugated anti-human CD13 (Biolegend), Pacific Blue conjugated anti-mouse/human CD11b (Biolegend), Biotin-conjugated anti-human CD16 (Biolegend) and V500-conjugated streptavidin (BD Bioscience, San Jose, CA, USA).

To analyze lymphoid cell lineage markers, cells were stained with a FITC-conjugated anti-human CD19 (Biolegend), PE-conjugated anti-human CD2 (Biolegend), APC-conjugated anti-human CD3 (Biolegend) and APC-Cy7-conjugated anti-human CD4 (Biolegend).

MOLM-13 and MV-4-11 cells: To analyze HSPC markers, cells were stained with a FITC-conjugated anti-human CD38, PE-conjugated anti-human CD33, PE-Cy7-conjugated anti-human c-KIT, APC-conjugated anti-human CD34 and Pacific Blue conjugated anti-human HLA-DR.

To analyze myeloid cell lineage markers, cells were stained with a FITC-conjugated anti-human CD15, PE-conjugated anti-mouse/human CD11b (Biolegend), PE-Cy7-conjugated anti-human CD14, APC-conjugated anti-human CD36 (Biolegend), APC-Cy7-conjugated anti-human CD13, Pacific Blue conjugated anti- human HLA-DR, Biotin-conjugated anti-human CD64 (Biolegend) and V500-conjugated streptavidin.

To analyze lymphoid cell lineage markers, cells were stained with a FITC-conjugated anti-human CD10 (Biolegend), PE-conjugated anti-human CD116, PE-Cy7-conjugated anti-human CD14, APC-conjugated anti-human CD11c Ab, APC-Cy7-conjugated anti-human CD4 (Biolegend), Pacific Blue conjugated anti-human HLA-DR, Biotin-conjugated anti-human CD45 (Biolegend) and V500-conjugated streptavidin.

K562 cells: To analyze HSPC markers, cells were stained with a FITC-conjugated anti-human CD38, PE-conjugated anti-human CD33, PE-Cy7-conjugated anti-human c-KIT, APC-conjugated anti-human CD34, APC-Cy7-conjugated anti-human CD13, and Pacific Blue conjugated anti-human HLA-DR.

To analyze erythroid cell lineage markers, cells were stained with a FITC-conjugated anti-human Glycophorin A (GPA, CD235a) (Biolegend), PE-conjugated anti- human CD71 (Biolegend), PE-Cy7-conjugated anti-human c-KIT, APC-conjugated anti-human CD36 (Biolegend), and APC-Cy7-conjugated anti-mouse/human CD44 (Biolegend).

Jurkat cells: To analyze HSPC markers, cells were stained with FITC-conjugated anti-human CD38, PE-conjugated anti-human CD33, PE-Cy7-conjugated anti-human c-KIT, and APC-conjugated anti-human CD34.

To analyze lymphoid cell lineage markers, cells were stained with FITC-conjugated anti-human CD7 (Biolegend), PE-conjugated anti-human CD2 (Biolegend), PE-Cy7-conjugated anti-human CD8 (Biolegend), APC-conjugated anti-human CD3 (Biolegend), APC-Cy7-conjugated anti-mouse/human CD4 (Biolegend), Pacific Blue conjugated anti-human CD5 (Biolegend), Biotin-conjugated anti-human CD38 and V500-conjugated streptavidin.

The cells were analyzed using a FACS Aria cell sorter (BDIS, San Jose, CA, USA), and the data files were analyzed using FlowJo software (Tree Star, Inc., Sac Carlos, CA, USA). Data are presented as means plus standard deviation (SD).

Quantitative real-time reverse transcription–polymerase chain reaction (qRT-PCR). Total RNA was extracted from each cell line

Table I. *Human leukemia cell lines*

Cell lines	Cell source	Type	Reference
Kasumi-1	Peripheral blood	Acute myeloblastic leukemia (M2)	7
NB4	Bone marrow	Acute promyelocytic leukemia (M3)	8
MOLM-13	Peripheral blood	Acute monocytic leukemia (M5a)	9
MV-4-11	Bone marrow/peripheral blood	Childhood acute myeloblastic leukemia (M5)	10
K562	Bone marrow	Chronic myelogenous leukemia/erythroleukemia	11
Jurkat	Peripheral blood	Acute T-cell leukemia	12

using an RNAqueous Micro Kit (Life Technologies, Carlsbad, CA, USA). Total RNA was subjected to reverse transcription using a High-Capacity RNA-to-cDNA Kit (Life Technologies) according to established protocols. The mRNA levels of different genes were analyzed by qRT-PCR using SYBR Green and gene-specific primers with the StepOnePlus real-time PCR system (Applied Biosystems, Foster City, CA, USA). The mRNA level of each target gene was normalized to β-actin (*ACTB*) as an internal control.

Results

Morphological observation of human leukemia cell lines. Leukemia cell lines used in this study are shown in Table I. To examine cell morphology, alive Propidium iodide (PI)-negative cells were sorted-out and stained with May-Grünwald Giemsa solution (Figure 1). Typical cell characteristics were observed under microscopy. Each cell line showed variations in size, nuclear segmentation, nuclear:cytoplasmic (N/C) ratio, and content of cytoplasm, such as granules and vacuoles. Kasumi cells (20.95±2.58 μm) showed nuclear segmentation (22.2%) in nuclei and vacuoles in the cytoplasm (85.7%). Azurophilic granules were contained inside the basophilic cytoplasm (Figure 1, upper left). No nuclear segmentation was observed in NB4 cells (24.49±2.91 μm) whose cytoplasm contained vacuoles (42.9%) with high N/C ratio. Azurophilic granules were contained in the basophilic cytoplasm (Figure 1, lower left). MOLM-13 cells (25.10±3.18 μm) did not have nuclear segmentation or vacuoles in the cytoplasm (42.8%). Azurophilic granules were contained in the basophilic cytoplasm (Figure 1, upper center). Nuclear condensation was observed in MV-4-11 cells (23.57±1.79 μm), but no nuclear segmentation or vacuoles in their cytoplasm were apparent (Figure 1, lower center). K562 cells (25.12±2.23 μm) also exhibited azurophilic granules in the basophilic cytoplasm (Figure 1, upper right). Compared to other cell lines, Jurkat cells were smaller in size (17.08±2.38 μm) and had a lower N/C ratio (Figure 1, lower right).

Surface marker expression of human leukemia cell lines. To further investigate surface marker expression of human leukemia cell lines, we performed flow cytometric analysis using HSPC markers such as c-KIT, CD34, CD33, CD38 for all cell lines; myeloid-specific markers such as CD45, CD13, CD14, CD15 for Kasumi-1, NB4, MOLM-13 and MV-4-11; erythroid-specific markers such as GPA, CD36, CD71 for K562 cells; and T-lymphocyte specific markers such as CD3, CD4, CD8 for Jurkat cells.

The percentages of positive cells for each marker are shown in Figure 2. The myelo/monoblastic leukemia cell lines, Kasumi-1, NB4, MOLM-13, and MV-4-11 were mostly positive for CD33 (HSPC marker) and CD45 (pan-leucocyte marker), in 99.8 to 100% and 98.9 to 99.6% of cells, respectively. Among them, Kasumi-1 cells were likely most immature, defined by positivity for c-KIT (99.8%) and CD34 (95.5%), and also expressed CD135 (2.2%). On the other hand, few NB4, MOLM and MV-4-11 cells were positive for CD34 (0.17 to 0.34%) and showed a variety of expression of CD38 (56.5%, 94.3%, 0.68%, respectively) and HLA-DR (19.6%, 23.4%, 85.0%, respectively). Regarding differentiation marker CD13 (pan-myeloid specific marker, widely expressed from Colony formings-granulocyte/macrophage (CFU-GM) equivalent cells to monocytes), NB4 cells were the ones most positive (99.8%), followed by Kasumi-1 cells (44.0%), MV-4-11 (5.38%) and MOLM-13 (1.32%) cells. NB4 cells showed the highest positivity for CD14 (30.4%), CD11b (80.4%) and CD11c (69.2%), and MV-4-11 did for CD15 (88.6%) and CD64 (99.6%) among the four cell lines (Figure 2). Erythroleukemia K562 cells had both immature state defined by c-KIT (12.9%) and CD33 (61.7%) expression and mature state defined by CD36 (75.3%), CD71 (99.8%) and GPA (19.7%). T-cell leukemia Jurkat cells were the most mature among the six cell lines tested, defined by c-KIT (1.22%). They were positive for markers of maturity: CD7 (pan-T-cell-specific marker, widely expressed from pro-T-cell to mature T-cell) in 60.9%, CD2 and CD5 (expressed from early thymocyte to mature thymocyte) as 59.0% and 57.0%, respectively, and CD3 and CD4 (mature T-cell marker) in 45.2% and 28.6%, respectively.

To further characterize the differentiated state of each cell line, we analyzed the surface marker expression under combination (Figure 3). All combination analyses are summarized in Table II. Kasumi-1 cells were double-positive for c-KIT/CD34 at 95.4%, CD33/HLA-DR at 7.4%, and

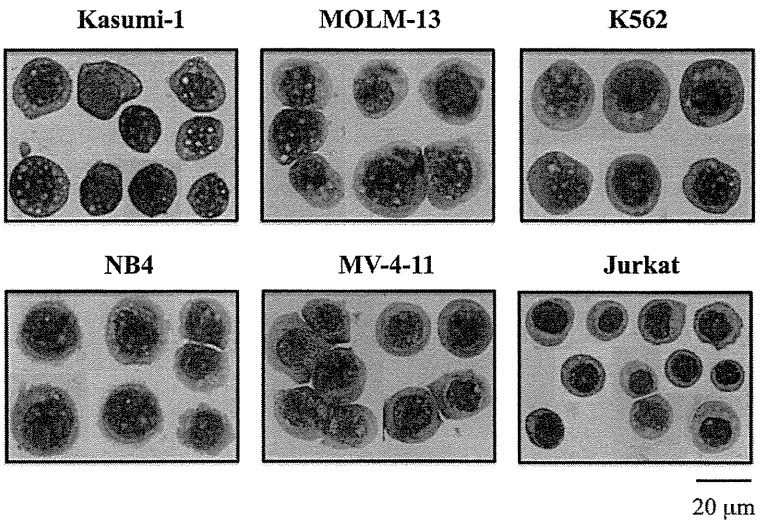

Figure 1. *Morphology of human leukemia cell lines. Morphology of Kasumi-1 (upper left), NB4 (lower left), MOLM-13 (upper center), MV-4-11 (lower center), K562 (upper right) and Jurkat (lower right) cells. All cell lines were stained with the May-Giemsa staining method. Original magnification, ×40 for all panels; scale bar is 20 μm.*

CD13/HLA-DR at 5.2%. Among CD13/CD116 double-positive (both are express from CFU-GM to mature monocytes), CD15-positive cells and CD11b-positive cells were observed at 2.12% and 64.6%, respectively, although we did not see cells highly positive for combinations CD14/CD15, CD15/CD16, CD11b/CD11c cells (Figure 3A). NB4 cells were double-positive for c-KIT/CD34, c-KIT/CD38, CD34/CD38 and c-KIT/HLA-DR cell at 0.06%, 14.4%, 2.6% and 2.7%, respectively. Regarding differentiation markers, positivity for CD15/CD116, CD11b/CD11c and CD14/CD11c cell were observed at 1.96%, 21.2% and 22.4%, respectively (Figure 3B). MOLM-13 cells were double-positive for c-KIT/CD38 and CD33/HLA-DR 9.83%, and 25.2%, but rarely for c-KIT/CD34. They were also positive for HLA-DR/CD13 cells at 2.2%. Compared to other cell lines, they were positive for single-cell markers, such as CD11b, CD14 and CD15, but no double-positivity was observed (Figure 3C). MV-4-11 cells were double-positive for CD33/HLA-DR at 85.8%, but rarely for c-KIT/CD34 and CD34/CD38. They were also positive for HLA-DR/CD13 at 0.9%. Regarding differentiation marker, CD15/CD64 were observed at 27.4%, but were rarely positive for CD14/CD116, CD36/CD63, and CD10/CD13 (Figure 3 D). K562 cells were double positive for c-KIT/CD33 and c-KIT/CD13 at 8.9% and 2.1%, but rarely for CD33/CD38, c-KIT/CD34 or HLA-DR/CD13. Among c-KIT-negative/CD36-positive cells that included Colony forming units-erythroid (CFU-E) equivalent cells, erythroblasts and mature erythrocytes, CD71/GPA double-positive polychromatic and CD44/GPA double-positive orthochromatic erythroblasts at 3.2% and 2.7% (Figure 3E). Jurkat cells were rarely double positive for CD33/CD34, c-KIT/CD34, CD34/CD38 cells and CD38/HLA-DR. Among double positive CD38/CD7 cells that are expected to include pro-T cell and thymocytes, CD2/CD5, CD3/CD4 and CD3/CD8 cells existed at 98.7%, 44.8%, and 1.2%. Among CD38-negative/CD7-positive cells that are expected to be mature, functional T-cells, double positive CD2/CD5 and CD3/CD4 cells were found at 94.6% and 36.0%, but were negative for CD3/CD8 (Figure 3F). Taken together from immunophenotype analysis, the differentiation state of Kasumi-1 and MOLM-13 cells appears to be CFU-GM to myeloblasts, NB4 cells are myeloblasts to pro-monocytes; MV-4-11 cells are myeloblasts; K562 cells are CFU-E to erythroblasts; and Jurkat cells are pro-T cells to mature thymocytes and functional T-cells.

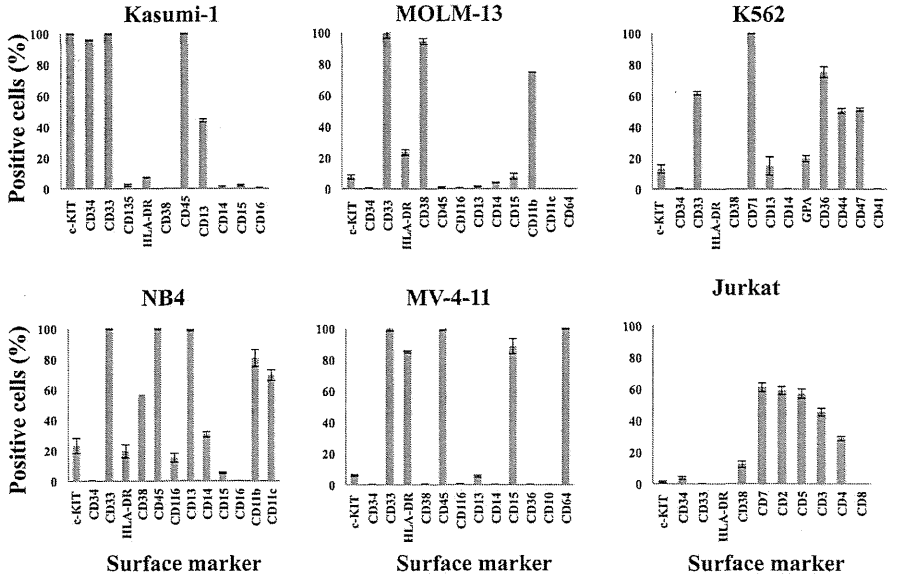

Figure 2. *Surface phenotype analysis with flow cytometry. Cells were stained with surface antigens, such as Tyrosine-protein kinase (c-KIT), Cluster of differentiation (CD) 34, CD33, CD38 and CD45, and analyzed with flow cytometry. Data are shown for each individual positive cell marker.*

Hematopoietic transcription factor expression in human leukemia cell lines. Next, we examined expression of hematopoietic transcription factor genes, such as *PU.1, CEBPα, GFI1, NOTCH1, E2A, GATA2, GATA1* and *FOG1* in six leukemia cell lines (Figure 4). Myeloblastic/ monoblastic cell lines (Kasumi-1, NB4, MOLM-13, and MV-4-11) express myeloid-specific transcription factors *PU.1* and *GFI1*. In contrast, CEBPα expression differed among cell lines, its expression in MV-4-11 was the highest and 9.45-fold higher in NB4 cells. Jurkat T-cell leukemia cells more highly expressed *NOTCH1* and *E2A* than did K562 erythroleukemia cell lines, at 8.09-fold and 6.82-fold higher, respectively. When compared to myeloblastic/monoblastic cell lines, Jurkat had the highest expression of both *NOTCH1* and *E2A*. K562 cells more highly expressed *GATA2* and *GATA1* than Jurkat cells, at 110.5-fold and 839.4-fold higher, respectively. When compared to myeloblastic/monoblastic cell lines, it had the highest expression of both *GATA2* and *GATA1* (Figure 4).

Among cell lines, Kasumi cells expressed *GFI1* (7837.28), *PU.1* (6010.33) and low expression of *CEBPα* (52.69). NB4 cells had higher expression of *CEBPα* (12699.06) than *PU.1* (7230.01) and *GFI1* (5565.11). MOLM-13 had higher expression of *PU.1* (11553.68) than *GFI1* (3848.21) and low expression of *CEBPα* (214.20). MV-4-11 predominantly expressed *CEBPα* (120013.11) and also expressed *PU.1* (11364.33) and GFI1 (4338.27). K562 cells predominantly expressed *GATA1* (1.2E+09) and also expressed *GATA2* (2432.562). Jurkat cells expressed 9.16-fold more *NOTCH1* than *E2A* (Figure 4). Overall, we found that the expression of hematopoietic transcription factors varies among leukemia cell lines at different levels.

Discussion

Herein, we carried-out multiple color analysis of cell surface markers by flow cytometry, and comparative analysis of expression of transcription genes on six human leukemia cell lines that are commonly used for studies on *in vitro* leukemic models. Our results suggest guidelines of standards for (i) quality control of cell lines, (ii) choosing appropriate cell lines for functional analysis, and (iii) determination of efficacy after functional analysis and drug screening.

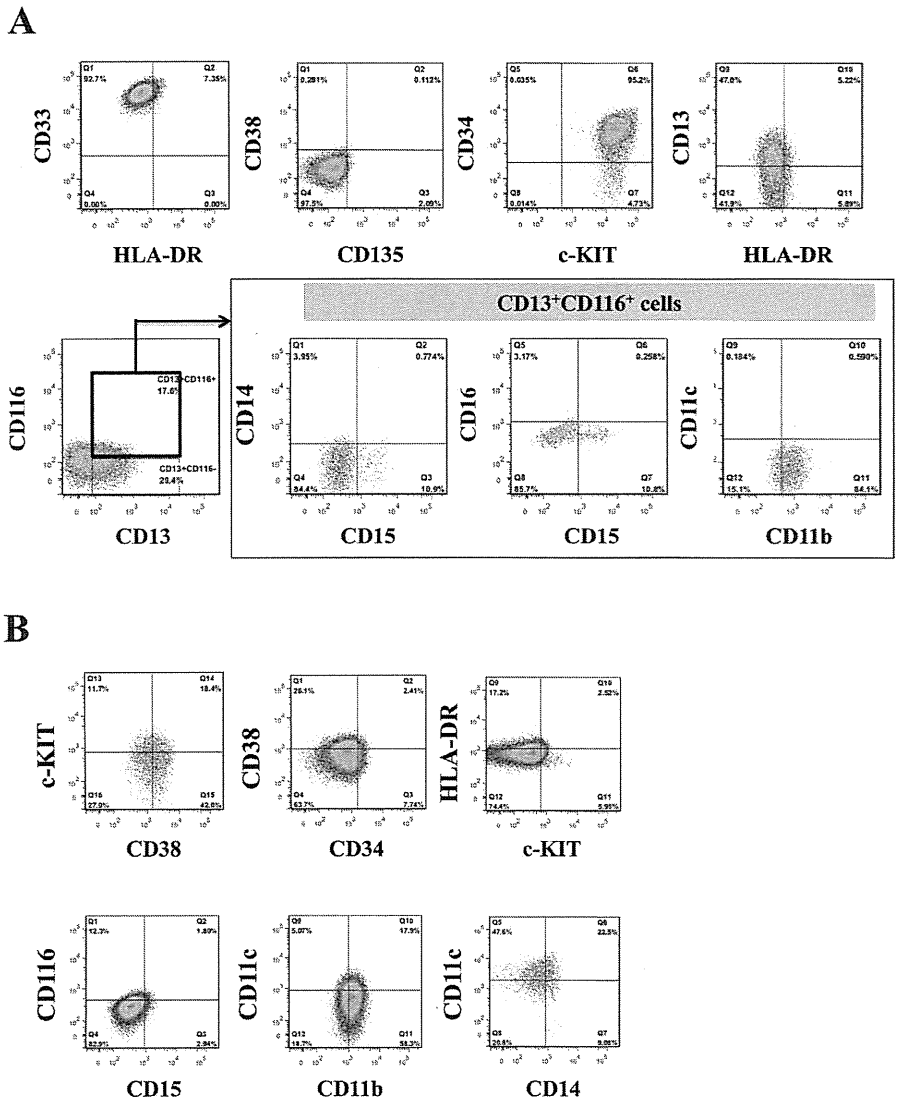

Figure 3. *Multiple color analysis of surface marker phenotype. Multiple color flow cytometric analyses were performed using Kasumi-1 (A), NB4 (B), MOLM-13 (C), MV-4-11 (D), K562 (E) and Jurkat (F) cells. Three independent flow cytometric analyses were carried-out in all cell lines and typical plot patterns are shown here.*

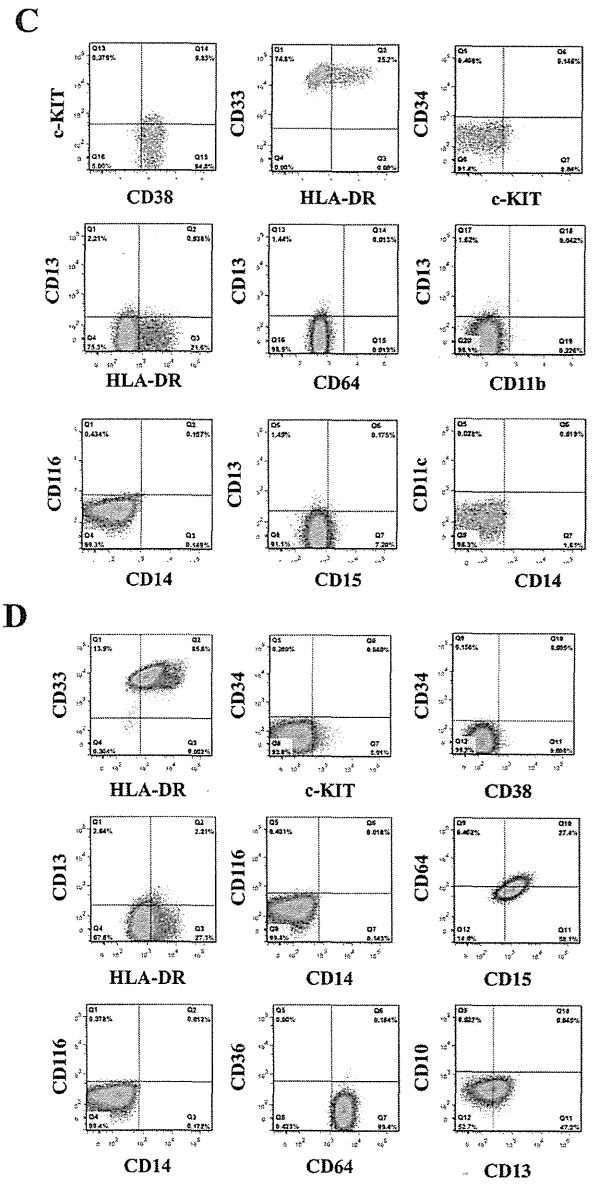

Figure 3. *Continued*

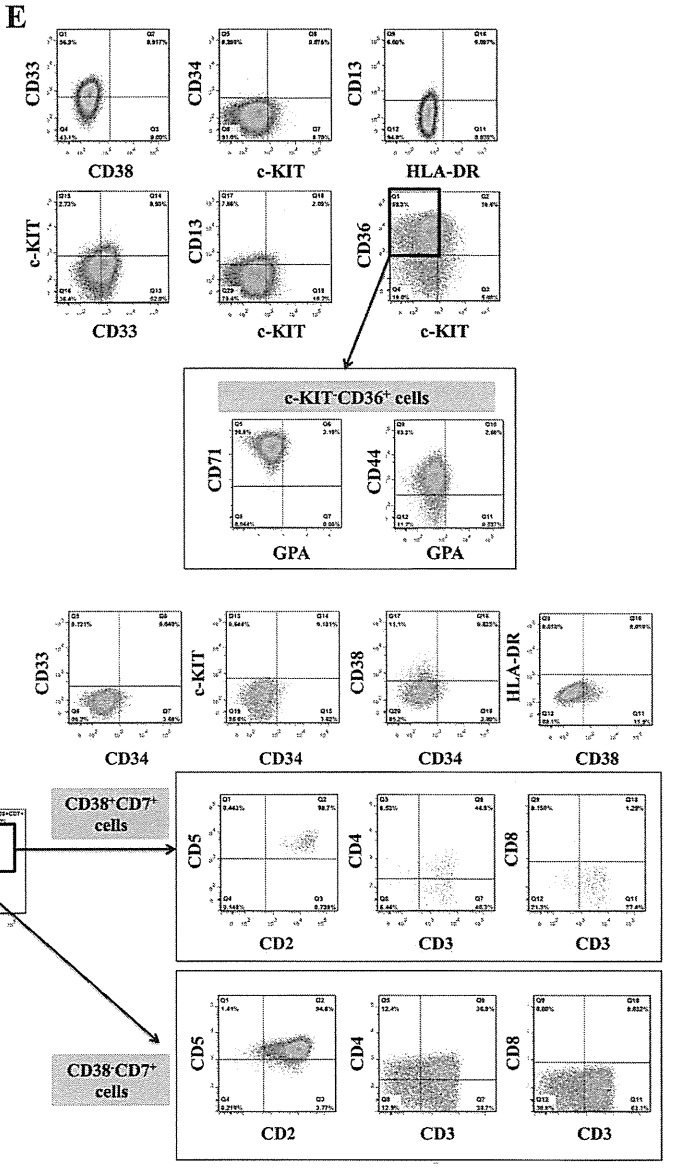

Figure 3. *Continued*